

# An Improved Method for Liver Diseases Detection by Ultrasound Image Analysis

Mehri Owjimehr, Habibollah Danyali, Mohammad Sadegh Helfroush

Department of Electrical and Electronics Engineering, Shiraz University of Technology, Shiraz, Iran

Submission: 01-03-2014

Accepted: 06-11-2014

## ABSTRACT

Ultrasound imaging is a popular and noninvasive tool frequently used in the diagnoses of liver diseases. A system to characterize normal, fatty and heterogeneous liver, using textural analysis of liver Ultrasound images, is proposed in this paper. The proposed approach is able to select the optimum regions of interest of the liver images. These optimum regions of interests are analyzed by two level wavelet packet transform to extract some statistical features, namely, median, standard deviation, and interquartile range. Discrimination between heterogeneous, fatty and normal livers is performed in a hierarchical approach in the classification stage. This stage, first, classifies focal and diffused livers and then distinguishes between fatty and normal ones. Support vector machine and k-nearest neighbor classifiers have been used to classify the images into three groups, and their performance is compared. The Support vector machine classifier outperformed the compared classifier, attaining an overall accuracy of 97.9%, with a sensitivity of 100%, 100% and 95.1% for the heterogeneous, fatty and normal class, respectively. The Acc obtained by the proposed computer-aided diagnostic system is quite promising and suggests that the proposed system can be used in a clinical environment to support radiologists and experts in liver diseases interpretation.

**Key words:** Automatic segmentation, fatty liver disease, hierarchical classification, wavelet packet transform

## INTRODUCTION

Fatty liver disease encloses a wide range of conditions that are characterized by triglyceride accumulation within the cytoplasm of hepatocytes and is related to obesity, insulin resistance, and metabolic syndrome. Fatty liver disease is one of the most common chronic hepatic diseases in all countries. It has been reported that the prevalence of fatty liver disease is as large as 20–30% in the general population of Middle East.<sup>[1]</sup>

Liver biopsy is considered as a diagnostic reference standard for the assessment of fatty infiltration of the liver. In biopsy, a small sample of tissue is taken from the liver using a needle.<sup>[2]</sup> This method is highly invasive and costly. However, medical imaging techniques such as ultrasound (US), computed tomography (CT) and magnetic resonance imaging are used for examination. As the US imaging is nonradiological, noninvasive, inexpensive, easy to operate and portable, it is a preferable diagnostic method for fatty liver. Extracting information from the fatty liver US images is based on the changes of scanned image intensity, which can be measured in the spatial domain.

Fatty liver causes an increase of echogenicity in the liver tissue. Echogenicity is the ability to create an echo that is, returning the signal in US examinations, and can be used to determine the brightness of US image.<sup>[3]</sup>

In order to help the physicians and experts diagnose and detect fatty liver disease, some authors recently proposed different schemes. Their schemes are based on computer-aided diagnosis (CAD).<sup>[3-10]</sup>

Liver segmentation, feature extraction, and classification are the main steps of CAD systems based on US imaging. There are several methods to segment a proper region of liver image. Most of them are manual, and a few others are semi-automatic and automatic. Manual approaches require medical experts to determine the regions of interest (ROI), before leaving to the computer for processing. Whereas, automated segmentation methods segment with minimal user input or without the need of any assistance from a medical expert. Authors of Wu *et al.*,<sup>[11]</sup> selected the ROI manually for each image in the patient database in the training phase. The threshold value to generate extremely stable edge pattern for the template image was then

### Address for correspondence:

Ms. Mehri Owjimehr, Department of Electrical and Electronics Engineering, Shiraz University of Technology, Shiraz, Iran.  
E-mail: m.owjimehr@sutech.ac.ir

learned. In the test phase, the ROI was detected based on a representative template using generalized Hough transform. Minhas *et al.*<sup>[7]</sup> a method was proposed to extract ROI semi-automatically. In training phase, some ROIs were extracted manually from the training US images to train the segmentation system. Then, the segmentation system extracted the final ROIs to be classified by classifier. The aim of the CAD systems is to minimize user intervention. Therefore, automatic approaches are preferred. However, the ROI selection Minhas *et al.*<sup>[7]</sup> and Wu *et al.*<sup>[11]</sup> is semi-automatic. An automatic ROI selection method was proposed in Ribeiro *et al.*<sup>[12]</sup> This method was used for the liver surface detection, based on decomposing the US images of the liver parenchyma into two fields: the speckled image containing textural information and the de-speckled image containing intensity and anatomical information of the liver. Features were extracted from the liver contour detected in the de-speckled field. The detected contour distinguished the liver anatomy from its neighbors, and the selected region was used as ROI. However, an efficient ROI should not include hepatic vessels, bile stores, and other anomalies. Therefore, the segmentation stage of this scheme may not be efficient due to the lack of anomalies removal.

Several approaches have been proposed for feature extraction in liver tissue based on US images. The most common features used for diagnosis of fatty liver are the first order and the second order statistical features based on texture analysis of the US images.<sup>[13,14]</sup> Texture analysis approaches can be divided into two groups: one based on the relation of neighbor pixels in spatial domain such as the gray level concurrence matrix (GLCM), the gray level difference statistical (GLDS), the gray level run length matrix (GLRLM) and fractal parameters (k); and one based on the analysis of transform coefficients such as Fourier power spectrum (FPS), discrete wavelet transform (DWT) and wavelet packet transform (WPT). The transform domain texture analyzers<sup>[7,15,16]</sup> have better performance than spatial domain ones<sup>[6,17-19]</sup> as texture characteristics are extracted more efficiently in transform domain. Among the explained texture analyzers in transform domain, WPT results in more independent and robust features since it performs a multi-resolution analysis in all frequency bands.

Finally, in the classification phase, different classifiers are proposed by researchers to discriminate normal and fatty livers, such as, artificial neural network (ANN),<sup>[6]</sup> probabilistic neural network (PNN),<sup>[18]</sup> self-organizing maps (SOM)<sup>[17]</sup> that is a kind of ANN with the ability of representing high-dimensional data, k-nearest neighbor (k-NN)<sup>[6,12]</sup> and support vector machine (SVM).<sup>[6,7,12,20,21]</sup>

The ANNs and the SVMs perform properly when a nonlinear relationship exists between the input and output features. These two classifiers have high speed of classification.

However, for neural network models and SVMs, a large sample size is required in order to achieve its maximum classification accuracy (Acc). The k-NN algorithms use space for training phase storage and in general k-NN and neural network are very sensitive to irrelevant features. As expected, neural networks and SVMs have more parameters than k-NN. The basic k-NN usually has only a single parameter which is relatively easy to tune.<sup>[22]</sup>

Mukherjee *et al.*<sup>[17]</sup> used GLCM to extract some statistical features from fatty liver US images, and then estimated the degree of distinction between normal and fatty clusters through texture analysis and SOM.

Andrade *et al.*<sup>[6]</sup> presented a semi-automatic classification approach to recognize fatty and normal liver. Several textural analysis models such as GLRLM, GLCM, and fractal dimension were used to extract features in three different classifiers, namely ANN, SVM, and k-NN. The Acc of 76.92% for ANN, 79.77% for SVM and 74.05% for k-NN classifiers were obtained.

Huang *et al.*<sup>[18]</sup> used three texture analysis methods, namely GLCM, gray level histogram and GLDS for textural analysis of liver in their work. Initially, image was de-noised, and different statistical features were extracted. Finally, PNN was applied to classify the normal and fatty liver with correct classification rate of 82.5% and 87.5% for normal and fatty classes, respectively.

Singh *et al.*<sup>[19]</sup> used some texture models including GLCM, FPS, and fractals and proposed a new metric based on the features to classify fatty and normal liver.

Yeh *et al.*<sup>[23]</sup> classified three grades of fatty liver with 25 MHz US images from liver samples obtained from surgical specimens. Their method was based on extracting feature from the GLCM and nonseparable DWT. The features extracted by both methods were used by SVM for classification with highest Acc of 90.5%.

Ribeiro *et al.*<sup>[15]</sup> proposed a classifier to discriminate normal and fatty livers. They used two important US features: liver parenchyma echogenicity and its texture. The acoustic attenuation coefficient was estimated by means of the slope of the linear regression of the mean image intensity along the depth direction (lines)<sup>[24]</sup> to apply echogenicity. In order to use texture features, energy and mean features were extracted from the first and second wavelet decomposition and some other features were extracted using autoregressive (AR) model coefficients corresponding to the coefficients of the first order two-dimensional AR model describing the image texture. Furthermore, WPT were employed to extract statistical features. Four types of classifiers, k-NN, Bayes and SVM (polynomial and radial-basis kernel) were applied to discriminate normal and

steatosis livers. The best-achieved result was observed for texture features, with the Bayes classifier, performing an Acc of 93.54% with a detection rate of 95.83% and 85.71% for normal and steatosis classes, respectively.

Minhas *et al.*<sup>[7]</sup> proposed a method to detect fatty and heterogeneous livers. The detected ROI was analyzed using WPT as textural analyzer, and a number of statistical features was obtained. Finally, a multi-class linear SVM was used for classification. Their approach led to an Acc of 95.4%.

Virmani *et al.*<sup>[16]</sup> proposed a CAD system for characterizing normal, cirrhotic and hepatocellular carcinoma (HCC) by the use of WPT texture descriptors and to extract mean, standard deviation, and energy features. Finally, SVM classifier was used to discriminate the three desired classes. The overall Acc of their approach is 88.8%.

Generally, fatty liver studies on CAD have concentrated on discriminating between healthy subjects and patients with fatty liver or other liver diseases based on manually selected ROIs. Furthermore, these studies have utilized one-against-all or one-against-one nonhierarchical classification schemes. Fully automatic selection of ROIs and hierarchical classification of liver diseases using US images have been paid less attention in computer-aided studies.

The aim of this study is to develop a noninvasive method based on the analysis of US images that not only accurately diagnose fatty and heterogeneous livers, but also automatically select the best ROIs from liver images.

As mentioned above, a fully automatic and efficient CAD system includes automatic selection of ROI, efficient feature extraction method and effective classification approach. In our proposed method, radiologist only determines the targets of the training stage and the ROIs are selected completely automatic without the need of radiologist's assistance. In this method, some ROIs have been selected by partitioning the US image, inspired by the clinical practice, and classification is performed by the use of these ROIs. This procedure presents a considerable low computational cost. Then the WPT is employed to extract some statistical features. Finally, in the classification part, we proposed a novel classification strategy based on a hierarchical method. The first stage of this method classifies heterogeneous liver from others and in the second stage discrimination of fatty and normal is performed.

The rest of this paper is organized as follows. The next section explains the main methodology. After, introducing the dataset used in this work, the procedure of selecting the ROIs is described. Then, texture analyzer and feature extraction are studied. Next section provides detailed information of classifiers. Finally, the results are presented, and the conclusion is reached.

## MATERIALS AND METHODS

In this method, after acquiring US images of the liver, few optimum ROIs are selected in the segmentation section. Then, WPT is applied to extract statistical features. Finally, a hierarchical classification approach is employed. Block diagram of the proposed method is illustrated in Figure 1.

### Image Acquisition

The US images of 88 subjects contain 30 fatty, 39 normal and 19 heterogeneous liver images. The images are of size  $560 \times 450$  pixels and saved in bitmap format. All images were obtained using a Toshiba SSA 550 digital B-mode US imaging system with a convex probe and at a 5 MHz tissue harmonic imaging frequency. The same dataset has been used in Minhas *et al.*<sup>[7]</sup> to enable us to have comparative results.

### SEGMENTATION

In order to have a CAD system, we would be looking for methods that avoid user intervention. Therefore, the purpose of this section is to select the proper ROI with an automatic method in the training and testing phases. It does not mean that an unsupervised method has been used in the training stage as in supervised method an expert determines the target of training samples. In fact, in our proposed approach, the proper ROIs are selected automatically without the use of any expert's assistance. However, the targets of training images are chosen by an expert.

In the proposed method, as illustrated in Figure 1, the US image of the liver is first cropped to extract a wide region near the central lobe and the black region around the main part is removed. This is performed in order to reduce the computational cost of the process.

Figure 2 shows a sample of the cropped image. The wide region is partitioned to 9 equal-size neighboring blocks as illustrated in Figure 3a. The partitioning continues to the next level, which 12 blocks are formed by overlapping the every two first level blocks, adjacent to each other both horizontally and vertically. This level is shown in Figure 3b and c. In the third level, 4 blocks are formed at the intersection of each four adjacent blocks of the first

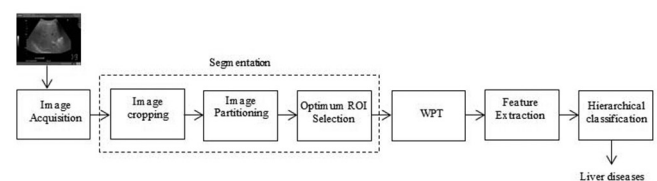


Figure 1: The block diagram of the proposed method

level as shown in Figure 3d. Finally, 25 equal overlapped blocks are specified. In order to find the proper ROIs, we select  $64 \times 64$ -pixel regions in the center of each block; therefore, 25 ROIs of size  $64 \times 64$ -pixels is obtained for each US image.

However, using all the ROIs in classification is not efficient and increases the computational cost. Therefore, a  $\nu$ -linear support vector classifier ( $\nu$ -LSVC)<sup>[25]</sup> is employed as a preprocessing stage, and after classification process, 8 ROIs, which have better results, are selected. The  $\nu$ -LSVC classifier is very fast and simple with low computational cost. Therefore, selection of the proper ROIs does not affect noticeably the computational cost and the speed of the training phase. Finally, these selected ROIs are used in the classification phase. The features that are used in this classification are explained in feature section.

### Wavelet Packet Transform

As mentioned in the introduction, feature extraction can be performed in the spatial and transform domains. Using texture descriptors in transform domain is much more reasonable in the sense that the human visual system processes images in a multi-scale way. Therefore, scale is a dominant aspect for analysis of texture.<sup>[16,26]</sup>

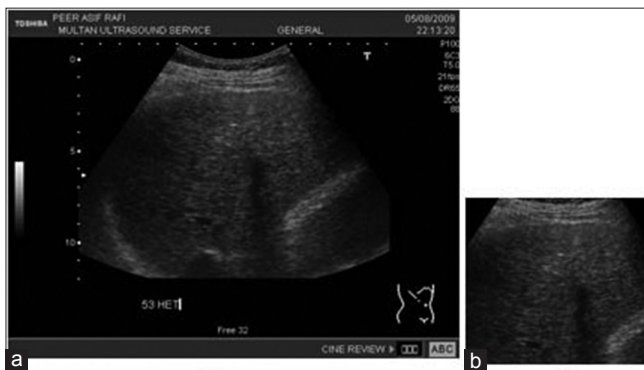


Figure 2: An example of the cropped liver ultrasound image

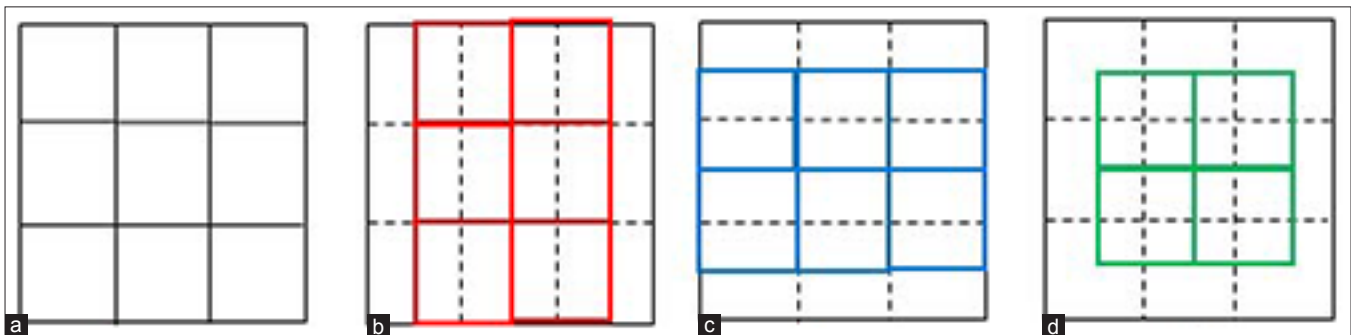


Figure 3: (a) The first level of partitioning (9 equal-size blocks), (b) and (c) The second level of partitioning (the process of forming 12 overlapped blocks at the intersection of two previous blocks in each row and in each column), (d) The third level of partitioning (the process of forming 4 overlapped blocks at the intersection of each four blocks of the first level)

In WPT, the image  $I(x, y)$  is decomposed into four subbands of approximation (a), horizontal (h), vertical (v) and diagonal (d) details at the first level and each of approximation and detail coefficients are decomposed further. This process is repeated to the desired level of decomposition. The WPT tree up to the second level of decomposition results in 16 subbands as shown in Figure 4. Figure 4b illustrates the WPT of an US image ROI at level 2 using the Daubechies3 wavelet. While DWT provides flexible time–frequency resolution, it suffers from a relatively low-resolution in the high-frequency parts. Differentiating high-frequency transient components becomes difficult and may not be efficient for texture characterization as most significant texture information usually appears in the middle and high-frequency bands, especially in texture with speckle noise. The WPT, in comparison, decomposes the detailed information of the image in the high-frequency parts.<sup>[27,28]</sup> The reason for using WPT for analysis of US images is that textural properties of the US image can be analyzed easily in the decomposed image at different frequency levels.

As Figure 4 shows, 4 and 16 subbands are obtained at the first and the second level of decomposition, respectively, which result totally in 20 subbands. The desired features are extracted from these 20 subbands. Moreover, we extract the features from the original ROIs. Therefore, features are extracted from both original ROIs in spatial domain and WPT subbands in transform domain.

### FEATURE EXTRACTION

The extracted features from WPT coefficients are median, standard deviation, and interquartile range. The median of the image shows the numerical value of intensity separating the higher half of pixel intensities in a window of the image from the lower half. The median value of intensity in US fatty liver images is higher than the intensity of normal ones due to their increased echogenicity caused by fat accumulation.<sup>[7]</sup> This characteristic also exists in WPT subbands of US fatty liver images. Standard deviation shows the variation from the mean. The interquartile range measures the dispersion

and is the difference between the upper and lower quartiles. The standard deviation and the interquartile range of the image represent the regularity or smoothness, of the US texture. These two features may be good indicators to distinguish US images of focal and diffused diseases of the liver. As a spatial domain feature, the ratio of the maximum to the minimum intensity value of pixels in the original ROI image in the spatial domain is computed as in.<sup>[7]</sup> Therefore, by calculating the three explained features from each of 20 subbands and one feature from the original ROI image in the spatial domain, feature vector of length 61 is obtained.

## CLASSIFICATION

This section aims to discriminate normal, fatty and heterogeneous livers. To reach this aim, a hierarchical classification scheme is proposed. A block diagram of this scheme is illustrated in Figure 5. The proposed hierarchical classification scheme is organized in two steps.

As already mentioned, in the normal case, both lobes of the liver are homogeneously clear and in the fatty case as it is a diffused disease, at least one lobe is accumulated homogeneously by fat. However, in a heterogeneous case a small region of the liver is only affected. Therefore, the fatty and normal cases can be placed in the diffused category and the heterogeneous case in the focal category. In order to have a hierarchical scheme, in the first classification step, focal case is discriminated from diffused case, if a liver is classified as diffused in the first step, discrimination of fatty and normal is examined in the second step.

Two types of classifiers, k-NN and SVM, are tested for the classification in each step. The purpose of SVM is to find a decision plane that has a maximum distance (margin) from the nearest training pattern.<sup>[29,30]</sup> In order to perform this aim, in some special cases, SVM maps the feature vector to a higher-dimensional space. In this space, the SVM finds

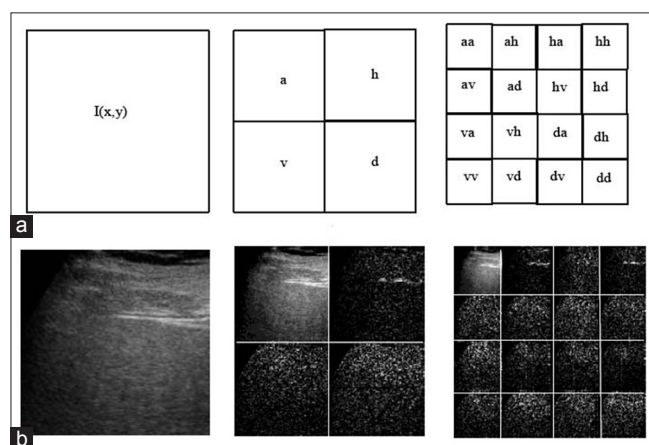


**Figure 4:** (a) Subband notation for 2 level wavelet packet transform (WPT) decomposition of image  $I(x, y)$ , (b) Decomposed liver ultrasound image after the first and the second level of WPT decomposition

a hyperplane to separate the two classes with a decision boundary set by support vectors.<sup>[29,30]</sup> An appropriate kernel function can increase the Acc of the classification process. In this paper, a binary SVM classifier is adopted using the polynomial kernel.

The k-NN classifier classifies a test sample according to the majority of its neighbors in the feature space using the minimum Euclidean distance criterion.<sup>[5,30]</sup>

To determine the optimal parameters for the classifiers, the different parameters are tested. The k-NN algorithm is implemented for values of  $k = 1, \dots, 9$  neighborhood configurations. The SVM is trained with a degree range of  $d = 1, \dots, 10$ . Only the best results are shown in this paper, which was obtained for  $k = 1$  and  $d = 2$ .

## RESULTS

In this section, the performance of the proposed method has been illustrated and evaluated. First, the evaluation criteria are explained and then the results are presented in three experiments. The first experiment uses leave one out cross validation (LOOCV) and one-against-all nonhierarchical method and evaluates the automatic selection of ROIs. The comparison between the proposed hierarchical scheme and one-against-all nonhierarchical method is performed in experiment 2. Finally, experiment 3 shows the performance of the proposed approach using 30% of dataset as test images and 70% as train images.

### Evaluation Criteria

The performance of the algorithm is investigated by sensitivity (Se), positive predictive value (PPV) and Acc.

### Automatic Selection of Regions of Interests

The first part of the implementation is selecting ROIs, which is performed as a fully automatic segmentation.

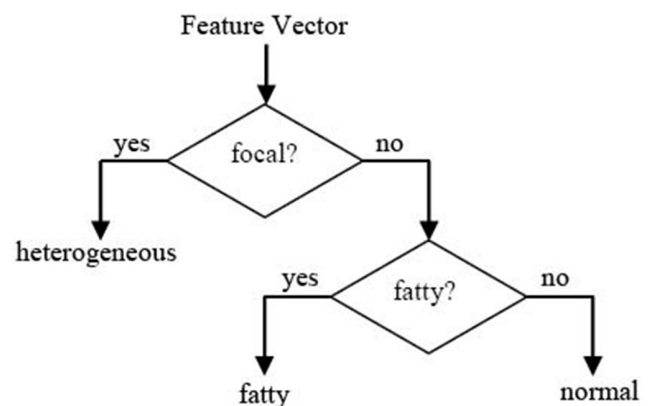


**Figure 5:** The proposed hierarchical classification scheme

The simplicity and reduction of computational cost of this method in comparison with the semi-automatic method of selecting ROI Minhas *et al.*,<sup>[7]</sup> without degrading the classification performance, is noticeable.

The first experiment contains a test over automatically selected ROIs and a comparison with the results of manually selected ROI. This test is performed on the 25 overlapped blocks. These blocks have the size of  $76 \times 84$  pixels. Totally, 25 ROIs are formed by selecting  $64 \times 64$ -pixel regions at the center of each block, and 8 optimum ROIs are selected as mentioned in the segmentation section. Each of these 8 ROIs is examined by SVM and k-NN classifiers. Therefore, eight-class labels are obtained for each liver image by each classifier. In this experiment, the one-against-all nonhierarchical scheme is employed to discriminate heterogeneous liver as Class 1, fatty liver as Class 2 and the normal one as Class 3. Finally, according to the eight-class labels, the majority vote rule determines the final class label.

### Hierarchical Classification

The second experiment is performed to show the effectiveness of the hierarchical classification scheme. This experiment contains a test over automatically selected ROIs, as in the first experiment, and a comparison with the results of Minhas *et al.*<sup>[7]</sup> At the first step of the classification, the diffused and focal classes are denoted as classes 1 and 2, respectively. At the second step, repeatedly, the fatty class is marked as Class 1 and the normal one as Class 2. The selected ROIs are examined by SVM and k-NN classifiers by the use of LOOCV method. Table 1 illustrates the Se and PPV of each class in each step and the Acc of each step.

### Select 30% of Dataset as Test Images

In the third experiment, the number of test samples is increased to evaluate this method more accurately. Therefore, the dataset is randomly partitioned to approximately 30% as test images and 70% as the training set. To reach this aim, the classification is performed using over 25 testing and 63 training images. This experiment is repeated with a hundred different random partitions in order to make any data bias associated with partitioning, insignificant. In this experiment, 25 overlapped blocks are used. The average of the Se and PPV of each class and Acc of each step of the system are shown in Table 2.

## DISCUSSION

The performance of classifiers in the first and the second experiments is evaluated by means of LOOCV method, same as the method used in Minhas *et al.*<sup>[7]</sup> to have a fair comparison with its results. This paper<sup>[7]</sup> is one of the most efficient and newest studies in classification of liver diseases and is the only study to discriminate fatty, normal

and heterogeneous livers. Minhas *et al.*<sup>[7]</sup> proposed an effective semi-automatic method to select a proper ROI in each US image.

Furthermore, this method is useful in cases with a small amount of available data as normally observed in medical problems. In LOOCV method, one case is left out as the testing set, and the rest of the data is used as the training set. This process is repeated so that each case is given a chance as the testing case.<sup>[31]</sup>

Tables 3 and 4 illustrate the Se and PPV of each class and the overall Acc using LOOCV method.

According to Table 3, the Se of 100% and 90.3% to detect the heterogeneous and fatty cases, respectively, shows the efficiency of the segmentation method. Furthermore, the PPVs of more than 90% represent efficient precision of the proposed scheme. Moreover, the results of this Table 3 illustrate the efficiency of SVM classifier compare to k-NN.

With the comparison between Tables 3 and 4, this experiment also illustrates that, using the automatically selected ROIs leads to better performance compared to the manually selected ROI. Moreover, in manually selected case, the results depend on the expert's assessment.

According to the results in Table 1, by considering 25 ROIs, this method is reliable and can be used in CAD systems in practical diagnosis of fatty and heterogeneous livers based on US images. As this Table 1 shows, the proposed method gives the Se of 100% for detecting both heterogeneous

**Table 1: Results of the one-against-all nonhierarchical scheme over 25 overlapped ROIs (automatic selection) by the use of leave one out cross validation**

Classifier labels	Sensitivity (%)		PPV (%)		Accuracy (%)	
	SVM	k-NN	SVM	k-NN	SVM	k-NN
Heterogeneous	100	80	80	63.2	91	82
Fatty	93.3	86.7	93.4	86.7		
Normal	86.4	79.1	97.4	87.2		

PPV – Positive predictive value; SVM – Support vector machine; k-NN – K-nearest neighbor; ROI – Regions of interest

**Table 2: Results of the one-against-all nonhierarchical scheme over manually selected ROI by the use of leave one out cross validation**

Classifier labels	Sensitivity (%)		PPV (%)		Accuracy (%)	
	SVM	k-NN	SVM	k-NN	SVM	k-NN
Heterogeneous	64.3	57.1	55	50.1	83.33	79.63
Fatty	78.8	76.9	86.7	66.7		
Normal	90.2	85.3	93.2	95.3		

PPV – Positive predictive value; SVM – Support vector machine; k-NN – k-nearest neighbor; ROI – Regions of interest

and fatty livers at the first and the second steps using SVM classifier. This shows the complete detection and quite correct diagnosis of these diseases, of course, for the available dataset.

Furthermore, we have achieved the overall Acc of 97.9% that is higher compared to the approach of Minhas *et al.*<sup>[7]</sup> with overall Acc of 95.4% in the same condition. In addition, the method of selecting ROIs in the proposed scheme is completely automatic with lower computational cost than the method of Minhas *et al.*<sup>[7]</sup> In the scheme of Minhas *et al.*<sup>[7]</sup> a medical expert had manually extracted ROIs from training US images. A given US image was first cropped to

**Table 3: Results of leave one out cross validation and hierarchical classification scheme for the third test (considering 25 overlapped blocks) in comparison with method of Minhas *et al.*<sup>[7]</sup>**

Classifier labels	Sensitivity (%)		PPV (%)		Accuracy (%)		Overall accuracy (%)	
	SVM	k-NN	SVM	k-NN	SVM	k-NN	SVM	k-NN
The proposed algorithm								
Step 1								
Focal (heterogeneous)	100	88.3	92.7	98.5	98.7	89.6	97.9	90.4
Diffused	96.1	90.91	100	72.6				
Step 2								
Fatty	100	95.7	93.3	90	97.1	91.3		
Normal	95.1	92.3	100	92.3				
Algorithm of <sup>[7]</sup> (using SVM classifier)								
Heterogeneous	94.7		100		N/A		95.4	
Fatty	93.3		93.3					
Normal	96.4		95					

PPV – Positive predictive value; SVM – Support vector machine; k-NN – k-nearest neighbor; ROI – Regions of interest

**Table 4: Average results of the third experiment by setting 30% of images as testing images and 70% as training images with hierarchical classification scheme and a comparison with results of 10 fold cross validation test of Minhas *et al.*<sup>[7]</sup>**

Classifier labels	Sensitivity %	PPV %	Accuracy %	Overall accuracy %
The proposed algorithm with 30% test and 70% train				
Step 1				
Focal (heterogeneous)	100	83.4	94.4	94.8
Diffused	95	100		
Step 2				
Fatty	95.5	100	95.2	
Normal	100	91.7		
Algorithm of <sup>[7]</sup> (10 fold cross validation)				
Heterogeneous	91	100	N/A	93.7
Fatty	92.4	92.4		
Normal	96.3	92.3		

PPV – Positive predictive value

extract a wide region near the central lobe. The continuous wavelet transform (CWT) of the cropped image was then taken with nine different scale parameter values. Thus, a single pixel of the original image could be represented as a nine-dimensional feature vector. As each of the manually selected ROI was  $64 \times 64$ -pixels, therefore, the total number of pixels available for training became 4,096 for a single ROI. Thus, the total number of examples for training the one class SVM for all the 88 images was 360,448. For efficient training of the one class SVM, the number of examples was reduced from 360,448 to 4,096 using k-means clustering. The cluster centers were then used to train the one-class SVM. For segmentation, the CWT of a given US image was taken, and the nine-dimensional representation of each pixel was subjected to the one-class SVM and some parameters were computed. After normalizing, applying morphological operations, filtering and finding the maximum value of pixels in each resulting image, the center of the proper ROI was found. Therefore, the method of ROI selection in Minhas *et al.*<sup>[7]</sup> is semi-automatic with high computational complexity. Moreover, their classification method is not a hierarchical one.

The results of Table 2 show that with increasing the number of test images up to 30%, the Acc changes by only a small amount. Furthermore, Se of 100% for heterogeneous and normal livers in steps 1 and 2 respectively, depicts the quite detection of these cases. Diagnosis of the fatty case is also performed with high Se of 95.5%. Moreover, the high PPVs, specially, 100% in the fatty case; illustrate perfect precision in diagnosing fatty liver disease. The overall Acc of 94.8% in this experiment shows the performance and robustness of the proposed algorithm in comparison with<sup>[7]</sup> in its 10 fold cross validation experiment with the Acc of 93.7%. Table 2 illustrates a comparison between our proposed algorithm in the third experiment and 10 fold cross validation test of Minhas *et al.*<sup>[7]</sup>

In addition to Minhas *et al.*<sup>[7]</sup> some other papers have proposed different approaches to classify normal and fatty liver or other liver diseases. However, a fair comparison between different methods and the proposed algorithm is complicated due to the differences in the type of liver diseases, datasets, the number of classes, the number of each class members in dataset, cross-validation technique and the evaluation criteria reported in the papers. The latest algorithms in the literature classify normal and fatty livers or stage the different grades of fatty liver, and the heterogeneous cases have been paid less attention. The results given in Huang *et al.*<sup>[18]</sup> show that their method gives a Se of 87.5% for detecting fatty liver. Their method uses 50 fatty, and 50 normal US liver images and selects ROIs manually. The approach in Zhou *et al.*<sup>[32]</sup> shows the Se of 81% in diagnosing fatty liver by the use of 52 normal and 69 fatty liver images and segmenting manually. The method given in Ribeiro *et al.*<sup>[15]</sup> represents the Se of 95.83% and 85.71% in detecting normal and fatty livers, respectively and an

overall Acc of 93.54%. Their algorithm uses 40 normal and 35 fatty liver images by manual ROI selecting. The method in Wang *et al.*<sup>[33]</sup> uses 24 normal and 59 fatty liver images and extracts two ROIs manually. This paper shows the Se of 92% in diagnosing fatty liver and the overall Acc of 88%. Table 5 shows a comparison between these algorithms.

## CONCLUSION

In this paper, an automatic segmentation and classification method to discriminate normal, fatty and heterogeneous liver images are proposed. The proposed algorithm is performed in two stages. The first stage, automatically selects some ROIs in a liver US image without the need of any assistance from a medical expert. The WPT is applied to the selected ROIs as a multi-scale texture analyzer to extract some statistical features. In the second stage, a hierarchical binary classification method using SVM classifier is employed. The proposed hierarchical classification algorithm discriminates the heterogeneous case from the diffused case at the first step and classifies fatty and normal cases at the second step. The overall Acc of 97.7% indicates the efficiency of the hierarchical classification scheme. The implementation results illustrate the suitability of the proposed system to be used in a clinical environment to help radiologists in liver disease classification and improve diagnostic Acc, which can avoid biopsies.

As mentioned already, fatty liver studies on CAD have focused on classification of healthy subjects and patients with fatty liver or different grades of it, as a consequence, one of the advantages of the proposed scheme in comparison with existing methods is that our approach considers discrimination between three different classes and detects heterogeneous cases, as in practice. Therefore, our proposed scheme is more usable in practical diagnosis than other existing approaches. The completely automatic scheme to

select the ROIs with the noticeable low computational cost is the other advantage of this system. This algorithm can be extended by enlarging the available database of liver images. Moreover, the proposed hierarchical method can be used in classifying different grades of fatty liver. Another interesting extension of the work can be to use other robust features based on Gabor filters or local binary pattern.

## REFERENCES

- Chalalani N, Younossi Z, Lavine JE, Diehl AM, Brunt EM, Cusi K, *et al.* The diagnosis and management of non-alcoholic fatty liver disease: Practice Guideline by the American Association for the Study of Liver Diseases, American College of Gastroenterology, and the American Gastroenterological Association. *Hepatology* 2012;55:2005-23.
- Ceylan R, Ceylan M, Özbay Y, Kara S. Fuzzy clustering complex-valued neural network to diagnose cirrhosis disease. *Expert Syst Appl* 2011;38:9744-51.
- Içer S, Coskun A, İkizceli T. Quantitative grading using grey relational analysis on ultrasonographic images of a fatty liver. *J Med Syst* 2012;36:2521-8.
- Suganya R, Rajaram S. Classification of liver diseases from ultrasound images using a hybrid kohonen SOM and LPND speckle reduction method. In *Signal Processing, Computing and Control (ISPC), 2012 IEEE International Conference on*, 2012. p. 1-6.
- Kadah YM, Farag AA, Zurada JM, Badawi AM, Youssef AM. Classification algorithms for quantitative tissue characterization of diffuse liver disease from ultrasound images. *IEEE Trans Med Imaging* 1996;15:466-78.
- Andrade A, Silva JS, Santos J, Belo-Soares P. Classifier approaches for liver steatosis using ultrasound images. *Procedia Technol* 2012;5:763-70.
- Minhas Fu, Sabih D, Hussain M. Automated classification of liver disorders using ultrasound images. *J Med Syst* 2012;36:3163-72.
- Mihailescu DM, Gui V, Toma CI, Popescu A, Sporea I. Automatic evaluation of steatosis by ultrasound image analysis. In *Electronics and Telecommunications (ISETC), 2012 10<sup>th</sup> International Symposium on*; 2012. p. 311-4.
- Yang Y, He Q, Hu C, Liao J, Meng MH. Method of edge energy template for detection of ultrasonic based fatty liver. In *Image and Signal Processing (CISP), 2010 3<sup>rd</sup> International Congress on*; 2010. p. 994-8.
- Moldovanu S, Moraru L, Bibicu D. Computerized decision support in liver steatosis investigation. *Int J Biol Biomed Eng* 2012;6:69-76.
- Wu YH, Lo YC, Cheng SC, Lin CL. Adaptive ultrasound image matching for automatic liver disease diagnosis using generalized hough transform. In *Intelligent Information Hiding and Multimedia Signal Processing (IIH-MSP), 2010 Sixth International Conference on*; 2010. p. 627-30.
- Ribeiro R, Marinho R, Velosa J, Ramalho F, Sanches JM. Diffuse liver disease classification from ultrasound surface characterization. Clinical and laboratorial data. In: eds. *Pattern Recognition and Image Analysis*. J. Vitria, J. M. Sanches and M. Hernandes. Berlin Heidelberg: Springer; 2011. p. 167-75.
- Wun YT, Chung R. Ultrasound characterization by stable statistical patterns. *Comput Methods Programs Biomed* 1998;55:117-26.
- Badawi AM, Derbala AS, Youssef AM. Fuzzy logic algorithm for quantitative tissue characterization of diffuse liver diseases from ultrasound images. *Int J Med Inform* 1999;55:135-47.
- Ribeiro R, Tato Marinho R, Sanches JM. Global and local detection of liver steatosis from ultrasound. In *Conference proceedings: Annual International Conference of the IEEE Engineering in Medicine and Biology Society. IEEE Engineering in Medicine and Biology Society. Conference*; 2012. p. 6547-50.

**Table 5: A comparison between the proposed algorithm and some new related algorithms**

Different approaches	Liver disease and number of dataset	Selecting ROI	Results %
Huang <i>et al.</i> <sup>[18]</sup>	Fatty (50) Normal (50)	Manually	Sensitivity: 87.5
Ribeiro <i>et al.</i> <sup>[15]</sup>	Fatty (40) Normal (35)	Manually	Accuracy: 93.54 Sensitivity (fatty): 85.71 Sensitivity (normal): 95.83
Zhou <i>et al.</i> <sup>[32]</sup>	Fatty (69) Normal (52)	Manually	Sensitivity: 81
Wang <i>et al.</i> <sup>[33]</sup>	Fatty (59) Normal (24)	Manually	Accuracy: 88 Sensitivity: 92
The proposed algorithm	Fatty (30) Normal (39) Heterogeneous (19)	Fully automatic	Accuracy: 97.9 Sensitivity (fatty): 100 Sensitivity (normal): 95.1 Sensitivity (heterogeneous): 100

ROI – Regions of interest



16. Virmani J, Kumar V, Kalra N, Khandelwal N. SVM-based characterization of liver ultrasound images using wavelet packet texture descriptors. *J Digit Imaging* 2013;26:530-43.
17. Mukherjee S, Chakravorty A, Ghosh K, Roy M, Adhikari A, Mazumdar S. Corroborating the subjective classification of ultrasound images of normal and fatty human livers by the radiologist through texture analysis and SOM. In *Advanced Computing and Communications, 2007. ADCOM 2007. International Conference on; 2007.* p. 197-202.
18. Huang Y, Han X, Tian X, Zhao Z, Zhao J, Hao D. Texture analysis of ultrasonic liver images based on spatial domain methods. In *Image and Signal Processing (CISP), 2010 3<sup>rd</sup> International Congress on; 2010.* p. 562-5.
19. Singh M, Singh S, Gupta S. A new measure of echogenicity of ultrasound images for liver classification. In *Electrical and Computer Engineering (CCECE), 2011 24<sup>th</sup> Canadian Conference on; 2011.* p. 000317-20.
20. Yeh WC, Jeng YM, Li CH, Lee PH, Li PC. Liver fatty change classification using 25 MHz high frequency ultrasound. In *Ultrasonics Symposium, 2004 IEEE; 2004.* p. 2169-72.
21. Ribeiro RT, Marinho RT, Sanches JM. Classification and staging of chronic liver disease from multimodal data. *IEEE Trans Biomed Eng* 2013;60:1336-44.
22. Kotsiantis SB, Zaharakis I, Pintelas P. Supervised machine learning: A review of classification techniques. *Informatica.* 31; 2007.
23. Yeh WC, Huang SW, Li PC. Liver fibrosis grade classification with B-mode ultrasound. *Ultrasound Med Biol* 2003;29:1229-35.
24. Gaitini D, Baruch Y, Ghersein E, Veitsman E, Kerner H, Shalem B, et al. Feasibility study of ultrasonic fatty liver biopsy: texture vs. attenuation and backscatter. *Ultrasound Med Biol* 2004;30:1321-7.
25. Chen PH, Lin CJ, Schölkopf B. A tutorial on v-support vector machines. *Appl Stoch Models Bus Ind* 2005;21:111-36.
26. Daugman JG. An information-theoretic view of analog representation in striate cortex. *Comput Neurosci* 1990;2:403-23.
27. Gao RX, Yan R. *Wavelets: Theory and Applications for Manufacturing.* Packet Transform. Springer; New York; 2010.
28. Chang T, Kuo CJ. Texture analysis and classification with tree-structured wavelet transform. *IEEE Trans Image Process* 1993;2:429-41.
29. Sudha S, Suresh G, Sukanesh R. Speckle noise reduction in ultrasound images using context-based adaptive wavelet thresholding. *IETE J Res* 2009;55:135.
30. Duda RO, Hart PE, Stork DG. *Pattern Classification.* New York; John Wiley and Sons; 2012.
31. Cawley GC, Talbot NL. Efficient leave-one-out cross-validation of kernel Fisher discriminant classifiers. *Pattern Recognit* 2003;36: 2585-92.
32. Zhou G, Wang Y, Wang W. Diagnosis of hepatic fibrosis by ultrasonic image analysis. In *Biomedical Engineering and Biotechnology (iCBEB), 2012 International Conference on; 2012.* p. 775-6.
33. Wang CY, Chen TB, Chen KF, Lu CY. Classification of nonalcoholic fatty liver ultrasonography by significant image features. In *Next-Generation Electronics (ISNE), 2013 IEEE International Symposium on; 2013.* p. 192-4.

**How to cite this article:** Owjimehr M, Danyali H, Helfroush MS. An Improved Method for Liver Diseases Detection by Ultrasound Image Analysis. *J Med Sign Sence* 2015;5:21-9.

**Source of Support:** Nil, **Conflict of Interest:** None declared

## BIOGRAPHIES



**Mehri Owjimehr** received the B.Sc. and M.Sc. degrees in communication engineering from Shiraz University, Shiraz, Iran, in 2008 and 2010. She is working toward the Ph.D. degree in communication in the Department of Telecommunication Engineering, Shiraz

University of Technology. Her primary research interests include data hiding and medical image processing.

**Email:** m.owjimehr@sutech.ac.ir



**Habibollah Danyali** received the B.Sc. and M.Sc. degrees in Electrical Engineering respectively from the Isfahan University of Technology, Isfahan, Iran, in 1991 and the Tarbiat Modarres University, Tehran, Iran, in 1993. In 2004, he received his

PhD degree in Computer Engineering from the University of Wollongong, Australia. He is with the Department of

Telecommunication Engineering, Shiraz University of Technology, Shiraz, Iran. His research interests include data hiding, scalable image and video coding.

**Email:** danyali@sutech.ac.ir



**Mohammad Sadegh Helfroush** received the B.S. and M.S. degrees in Electrical engineering from Shiraz University of Shiraz and Sharif University of Technology, Tehran in 1993 and 1995, respectively. He performed his Ph.D. degree in Electrical

Engineering from Tarbiat Modares University, Tehran, Iran. Actually he is working as associate professor in department of Electrical and Electronics Engineering, Shiraz University of Technology, Shiraz, Iran.

**Email:** ms\_helfroush@sutech.ac.ir